

DEEP NITSCHKE METHOD: DEEP RITZ METHOD WITH ESSENTIAL BOUNDARY CONDITIONS

YULEI LIAO AND PINGBING MING

ABSTRACT. We propose a method due to Nitsche (Deep Nitsche Method) from 1970s to deal with the essential boundary conditions encountered in the deep learning-based numerical method without significant extra computational costs. The method inherits several advantages from Deep Ritz Method [6] while successfully overcomes the difficulties in treatment of the essential boundary conditions. We illustrate the method on several representative problems posed in at most 100 dimensions with complicated boundary conditions. The numerical results clearly show that the Deep Nitsche Method is naturally nonlinear, naturally adaptive and has the potential to work on rather high dimensions.

1. INTRODUCTION

Recently there is a surge of interest in solving partial differential equations by deep learning-based numerical methods [5, 11, 6, 9, 15, 2]. However, there are few attempts to deal with the boundary conditions, particularly the essential boundary conditions, which is the main objective of the present work. These methods allow for the compositional construction of new approximation spaces from various neural networks. Such constructions are usually free of a mesh so that they are in essence *meshless methods*. The shape functions in the approximation spaces are in general non interpolatory, which makes the implementation of the essential boundary conditions not an easy task. Many approaches toward dealing with the essential boundary conditions have been proposed over the past fifty years; we refer to [1, §7.2] for a review.

In fact, an efficient method for imposing the essential boundary conditions has been proposed by Nitsche in the early 1970s [14]. This method was revived to deal with the elliptic interface problems and the unfitted mesh problems; we refer to [4] for a review of the progress in this direction. In the context of the meshless method, Nitsche's idea has been proved to be an efficient approach to deal with boundary conditions in the framework of partition of unity method [8] as well as

Date: December 4, 2019.

Key words and phrases. Deep Ritz Method, Neural Network Approximation, Curse of Dimensionality.

This work was supported by the National Natural Science Foundation of China for Distinguished Young Scholars 11425106, and this work is also supported by Beijing Academy of Artificial Intelligence (BAAI).

generalized finite element method [1]. In this work, we incorporate the idea of Nitsche to deal with the essential boundary conditions in the framework of Deep Ritz Method [6]. We call this new algorithm the Deep Nitsche Method. In the next part, we introduce the energy formulation of the method, and then we present the numerical results for solving some mixed boundary value problems with regular and singular solutions in two dimensions and also for problems in high dimensions up to 100. In particular, we compare Deep Nitsche Method with Deep Ritz Method and another method based on least-squares variational formulation in all the examples. Finally we conclude with some remarks.

2. DEEP NITSCHKE METHOD

We consider the mixed boundary value problem posed on $\Omega \subset \mathbb{R}^d$:

$$(2.1) \quad \begin{cases} -\nabla \cdot (A \nabla u) = f, & \text{in } \Omega, \\ u = g_D, & \text{on } \Gamma_D, \\ (A \nabla u) \cdot n = g_N, & \text{on } \Gamma_N, \end{cases}$$

where $A \in \mathbb{R}^{d \times d}$ is a symmetrical matrix satisfying

$$\lambda \sum_{i=1}^d \xi_i^2 \leq \sum_{i,j=1}^d A_{ij}(x) \xi_i \xi_j \leq \Lambda \sum_{i=1}^d \xi_i^2 \quad \text{for a.e. } x \in \Omega \quad \text{and} \quad (\xi_1, \dots, \xi_d) \in \mathbb{R}^d.$$

The boundary $\Gamma_D \cup \Gamma_N = \partial\Omega$ and $\bar{\Gamma}_D \cap \bar{\Gamma}_N \neq \emptyset$.

The energy functional associated with the above boundary value problem in the sense of Nitsche [14] is

$$(2.2) \quad \begin{aligned} I[v] := & \frac{1}{2} \int_{\Omega} A \nabla v \cdot \nabla v \, dx - \int_{\Gamma_D} v A \nabla v \cdot n \, d\sigma(x) + \frac{\beta}{2} \int_{\Gamma_D} v^2 \, d\sigma(x) \\ & - \int_{\Omega} f v \, dx - \int_{\Gamma_D} g_D (\beta v - A \nabla v \cdot n) \, d\sigma(x) - \int_{\Gamma_N} g_N v \, d\sigma(x), \end{aligned}$$

where β is a parameter to be determined later on. We minimize $I[v]$ over certain trial space \mathcal{H} that will be defined later on. The resulting optimization problem is solved by the Stochastic Gradient Decent (SGD) method [7, §8].

$$(2.3) \quad \hat{u} = \operatorname{argmin}_{v \in \mathcal{H}} I[v].$$

The associated variational problem is: find $\hat{u} \in \mathcal{H}$ such that

$$(2.4) \quad a(\hat{u}, v) = \ell(v) \quad \text{for all } v \in \mathcal{H},$$

where the bilinear form a and the linear functional ℓ are defined by

$$a(u, v) := \int_{\Omega} A \nabla u \cdot \nabla v \, dx + \int_{\Gamma_D} (u (\beta v - (A \nabla v) \cdot n) - v (A \nabla u) \cdot n) \, d\sigma(x),$$

for all $u, v \in \mathcal{H}$, and

$$\ell(v) := \int_{\Omega} f v \, dx + \int_{\Gamma_D} g_D (\beta v - A \nabla v \cdot n) \, d\sigma(x) + \int_{\Gamma_N} g_N v \, d\sigma(x) \quad v \in \mathcal{H},$$

respectively.

To prove the well-posedness of (2.4), we need prove the coercivity of a , and the boundedness of a and ℓ . We make the following

Assumption: There exists a constant C_{inv} such that for all $v \in \mathcal{H}$,

$$(2.5) \quad \|\nabla v\|_{L^2(\Gamma_D)} \leq C_{\text{inv}} \|\nabla v\|_{L^2(\Omega)}.$$

Define a norm

$$\|v\|^2 := \|\nabla v\|_{L^2(\Omega)}^2 + \|v\|_{L^2(\Gamma_D)}^2.$$

By Friedrich's inequality, $\|\cdot\|$ is equivalent to the standard H^1 -norm.

Lemma 2.1. *Let **Assumption 2.5** is valid and if $\beta > 2\Lambda^2 C_{\text{inv}}^2 / \lambda$, then*

$$(2.6) \quad a(v, v) \geq \tilde{\lambda} \|v\|^2 \quad \text{for all } v \in \mathcal{H},$$

where $\tilde{\lambda} = \min(\lambda - 2\Lambda^2 C_{\text{inv}}^2 / \beta, \beta/2)$.

Proof. For any $v \in \mathcal{H}$,

$$a(v, v) \geq \lambda \int_{\Omega} |\nabla v|^2 dx + \beta \int_{\Gamma_D} v^2 d\sigma(x) - 2 \int_{\Gamma_D} v(A\nabla v) \cdot n d\sigma(x).$$

Using Cauchy-Schwartz inequality and the assumption (2.5), we obtain

$$\begin{aligned} \left| \int_{\Gamma_D} v(A\nabla v) \cdot n d\sigma(x) \right| &\leq \Lambda \|v\|_{L^2(\Gamma_D)} \|\nabla v\|_{L^2(\Gamma_D)} \\ &\leq \frac{\beta}{4} \|v\|_{L^2(\Gamma_D)}^2 + \frac{\Lambda^2}{\beta} \|\partial_n v\|_{L^2(\Gamma_D)}^2 \\ &\leq \frac{\beta}{4} \|v\|_{L^2(\Gamma_D)}^2 + \frac{\Lambda^2 C_{\text{inv}}^2}{\beta} \|\nabla v\|_{L^2(\Omega)}^2. \end{aligned}$$

Combining the above two equations, we obtain (2.6). \square

The boundedness of a and ℓ may be proved in a similar way. The well-posedness of the variational problem boils down to the inverse assumption (2.5), which is natural for the case when \mathcal{H} consists of polynomials, i.e.,

$$\|\nabla v\|_{L^2(\Gamma_D)} \leq Ch^{-1/2} \|\nabla v\|_{L^2(\Omega)},$$

where h is the mesh size of the triangulation. This means that we need to take $\beta = c_0 h^{-1}$ for certain large c_0 , such choice is standard in finite element literature. However, we do not know whether such *inverse inequality* is true for functions in \mathcal{H} that are constructed from various neural networks in compositional manner. The only exception is the function constructed from the Gaussian networks [13], which does not seem apply to the present case because it employ the distance between the centers as a measure of discretization.

The trial functions space \mathcal{H} is modeled by ResNet [10]. The component of ResNet is shown in Figure 1. The input layer is a fully connected layer with m hidden nodes,

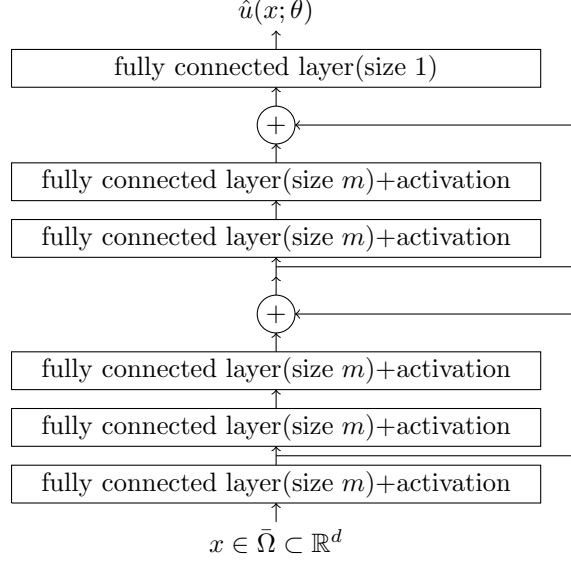


FIGURE 1. The component of ResNet

which maps x from \mathbb{R}^d to \mathbb{R}^m . Assume that σ is a scalar activation function and let ϕ be the tensor product of σ as $\phi(x) = (\sigma(x_1), \dots, \sigma(x_m)) \in \mathbb{R}^m$, then

$$s_1 = \phi(W_1 x + b_1),$$

where $W_1 \in \mathbb{R}^{m \times d}$, $b_1 \in \mathbb{R}^m$. The hidden layers is constructed by l residual blocks. Each block contains two fully connected layers and one residual connection layer. The i -th block takes the form

$$s_{i+1} = \phi(W_{2,i} \phi(W_{1,i} s_i + b_{1,i}) + b_{2,i}) + s_i,$$

where $W_{1,i}, W_{2,i} \in \mathbb{R}^{m \times m}$ and $b_{1,i}, b_{2,i} \in \mathbb{R}^m$.

The output layer is a fully connected layer with one hidden node. The approximation solution may be expressed as

$$\hat{u}(x; \theta) = W_2 s_{l+1} + b_2,$$

where $W_2 \in \mathbb{R}^{1 \times m}$ and $b_2 \in \mathbb{R}$, the parameter set θ is defined as

$$\theta = \{ W_1, W_2, b_1, b_2, W_{1,i}, W_{2,i}, b_{1,i}, b_{2,i} \mid i = 1, \dots, l \}.$$

In each step of the SGD iteration, we randomly sample N_i points $\{x_k^{(i)}\}_{k=1}^{N_i} \subset \Omega$, N_d points $\{x_k^{(d)}\}_{k=1}^{N_d} \subset \Gamma_D$ and N_n points $\{x_k^{(n)}\}_{k=1}^{N_n} \subset \Gamma_N$. The loss function is

defined as

$$\begin{aligned} \text{Loss} = & \frac{|\Omega|}{N_i} \sum_{k=1}^{N_i} \left(\frac{1}{2} A(x_k^{(i)}) \nabla_x \hat{u}(x_k^{(i)}; \theta) \cdot \nabla_x \hat{u}(x_k^{(i)}; \theta) - f(x_k^{(i)}) \hat{u}(x_k^{(i)}; \theta) \right) \\ & + \frac{|\Gamma_D|}{N_d} \sum_{k=1}^{N_d} \left(\frac{\beta}{2} \hat{u}^2(x_k^{(d)}; \theta) - \hat{u}(x_k^{(d)}; \theta) A(x_k^{(d)}) \nabla_x \hat{u}(x_k^{(d)}; \theta) \cdot n \right) \\ & - \frac{|\Gamma_D|}{N_d} \sum_{k=1}^{N_d} g_D \left(\beta \hat{u}(x_k^{(d)}; \theta) - A(x_k^{(d)}) \nabla_x \hat{u}(x_k^{(d)}; \theta) \cdot n \right) \\ & - \frac{|\Gamma_N|}{N_n} \sum_{k=1}^{N_n} g_N \hat{u}(x_k^{(n)}; \theta). \end{aligned}$$

3. NUMERICAL EXPERIMENTS

We apply the Deep Nitsche Method to solve the mixed boundary value problem (2.1), and compare it with two known methods such as Deep Ritz Method in [6] and a deep learning-based least-squares method [15], which at least dates back to [3] in finite element method. The energy functional associated with boundary value problem (2.1) for Deep Ritz Method reads as

$$I[v] = \int_{\Omega} \left(\frac{1}{2} A \nabla v \cdot \nabla v - f v \right) dx + \beta \int_{\Gamma_D} (v - g_D)^2 d\sigma(x) - \int_{\Gamma_N} g_N v d\sigma(x),$$

and the energy functional associated with the Least-squares is

$$I[v] = \int_{\Omega} (\nabla \cdot (A \nabla v) + f)^2 dx + \beta \int_{\Gamma_D} (v - g_D)^2 d\sigma(x) + \beta \int_{\Gamma_N} (A \nabla \cdot n - g_N)^2 d\sigma(x).$$

In all the examples, we let Ω be the unit hypercube as $\Omega = (0, 1)^d$ and the activation function $\sigma = \tanh$.

3.1. Two dimensional examples. The solution u is approximated by a neural network with five residual blocks and ten hidden nodes per fully connected layer. Noticing that one residual block contains two fully connected layers and one residual connection, the number of trainable parameters is 1141. An Adam optimizer is employed to train with the learning rate 0.001 [12]. We train the model for 50000 epochs. In each epoch, we randomly sample 128 points inside the domain Ω and 33 points on each edge of $\partial\Omega$.

In the first example, we solve the Laplace equation with a smooth solution

$$u(x, y) = \cos(\pi x) \sin(\pi y).$$

The boundary $\Gamma_D = (0, 1) \times \{0, 1\}$ and $\Gamma_N = \{0, 1\} \times (0, 1)$ and we compute f , g_D and g_N by (2.1). We report the relative errors

$$e_{L^2} := \frac{\|u - \hat{u}\|_{L^2}}{\|u\|_{L^2}}, \quad e_{H^1} := \frac{\|u - \hat{u}\|_{H^1}}{\|u\|_{H^1}}, \quad e_{H^2} := \frac{\|u - \hat{u}\|_{H^2}}{\|u\|_{H^2}}$$

in Table 1 for three methods with different penalized parameters β .

TABLE 1. The smooth solution in $d = 2$

β	e_{L^2}	e_{H^1}	e_{H^2}
Deep Nitsche Method			
50	3.948e-2	6.668e-2	2.111e-1
500	6.492e-2	6.782e-2	1.585e-1
5000	2.029e-2	4.135e-2	1.569e-1
50000	1.270e-1	2.041e-1	4.592e-1
Deep Ritz Method			
50	2.732e-2	4.822e-2	1.136e-1
500	1.068e-2	3.069e-2	1.143e-1
5000	5.154e-2	1.008e-1	2.933e-1
50000	9.642e-1	9.663e-1	9.489e-1
Least-Squares Method			
50	5.086e-3	2.995e-3	4.570e-3
500	4.160e-3	2.564e-3	6.857e-3
5000	5.787e-3	9.322e-3	2.965e-2
50000	4.946e-2	5.909e-2	1.174e-1

It seems all three methods give comparable accuracy, and the difference between the errors with parameter β varying from 50 to 5000 are negligible, while β with very big value seems a bad choice. It is worthwhile to mention that $\beta = 5000$ seems the best for the Deep Nitsche method, while $\beta = 500$ seems the best for the Deep Ritz method and the least-squares method.

In the second example, we consider

$$\begin{cases} -\Delta u(x) = 0, & x \in \Omega, \\ u(x) = u(r, \theta) = r^{1/2} \sin(\theta/2), & x \in \partial\Omega, \end{cases}$$

where $\Omega = (-1, 1)^2 \setminus [0, 1)^2$ is an L-shaped domain. This problem admits an analytical solution $u(x) = u(r, \theta) = r^{1/2} \sin(\theta/2)$, which belongs to $H^s(\Omega)$ with $s < 3/2$. In fact, such solution usually stands for the singular part of the general situation [16]. We report the errors in Table 2. We have not computed the error in H^2 norm because $\|u\|_{H^2}$ is obviously unbounded. In view of Table 2, it seems that all three methods are robust with respect to the parameter β , and Deep Nitsche method seems the most accurate method for approximating the singular solution.

In the last example in two dimensions, we test problem with a nonconstant coefficient matrix A . The set up is the same with the previous example. Let

$$A = \begin{pmatrix} (x+1)^2 + y^2 & -xy \\ -xy & (x+1)^2 \end{pmatrix},$$

TABLE 2. The singular solution in L -domain

β	e_{L^2}	e_{H^1}
Deep Nitsche Method		
50	7.070e-3	8.211e-2
500	7.570e-3	9.107e-2
5000	1.730e-2	1.885e-1
50000	4.959e-2	2.993e-1
Deep Ritz Method		
50	1.055e-2	7.565e-2
500	9.487e-3	1.124e-1
5000	1.982e-2	2.011e-1
50000	6.542e-2	4.783e-1
Least-Squares Method		
50	1.530e-2	1.170e-1
500	6.755e-3	1.015e-1
5000	2.145e-2	1.241e-1
50000	7.434e-2	1.951e-1

and

$$u(x, y) = x^3 y^2 + x \sin(2\pi xy) \sin(2\pi y),$$

where $\Gamma_D = \{1\} \times (0, 1) \cup (0, 1) \times \{1\}$ and $\Gamma_N = \{0\} \times (0, 1) \cup (0, 1) \times \{0\}$. We calculate f , g_D and g_N according to (2.1). The relative errors e_{L^2} , e_{H^1} and e_{H^2} are reported in Table 3.

In view of Table 3, it seems all methods are quite robust with respect to the penalized parameter, and the least-squares gives the best results even in case of large β .

3.2. High dimensional examples. We turn to problems in high dimensions in this part. We still employ an Adam optimizer with the learning rate 0.001 and train the model for 50000 epochs. In each epoch, we randomly sample 512 points in Ω and 16 points on each face of $\partial\Omega$.

In the first example, we consider a less smooth solution in 20 dimensions

$$u(x) = \left(\sum_{i=1}^{20} x_i^2 \right)^{5/2}, \quad x \in (0, 1)^{20}$$

with a pure Dirichlet boundary condition. We calculate f and g_D by (2.1). This example has been test in [8] with a particle-partition of unit method. We approximate the solution by a neural network with five residual blocks and 50 hidden nodes per fully connected layer. Thus the number of trainable parameters is 26601. We report the relative errors in Table 4.

TABLE 3. Results for problem with coefficient in $d = 2$

β	e_{L^2}	e_{H^1}	e_{H^2}
Deep Nitsche Method			
50	3.940e-1	7.923e-1	1.156e0
500	6.121e-2	7.416e-2	2.011e-1
5000	2.441e-2	6.358e-2	1.768e-1
50000	6.902e-2	1.463e-1	3.587e-1
Deep Ritz Method			
50	8.901e-2	1.063e-1	2.068e-1
500	3.945e-2	6.079e-2	1.737e-1
5000	4.272e-2	1.106e-1	4.919e-1
50000	1.951e-1	3.235e-1	5.667e-1
Least-Squares Method			
50	2.593e-2	5.821e-2	7.888e-2
500	1.345e-2	3.282e-2	5.881e-2
5000	3.658e-2	3.564e-2	5.888e-2
50000	8.185e-2	5.413e-2	7.555e-2

TABLE 4. Less smooth solution in 20 dimensions

β	e_{L^2}	e_{H^1}	e_{H^2}
Deep Nitsche Method			
50	1.962e-2	6.887e-2	2.186e-1
500	2.517e-2	8.051e-2	5.411e-1
5000	1.584e-2	6.112e-2	4.659e-1
50000	2.098e-2	7.653e-2	3.837e-1
Deep Ritz Method			
50	2.102e-2	5.902e-2	3.962e-1
500	1.215e-2	4.788e-2	3.831e-1
5000	1.351e-2	5.612e-2	1.553e-1
50000	1.102e-2	4.650e-2	4.424e-1
Least-Squares Method			
50	4.486e-2	7.156e-2	1.861e-1
500	1.434e-2	5.442e-2	1.921e-1
5000	2.049e-2	5.484e-2	2.103e-1
50000	1.242e-2	4.704e-2	2.333e-1

In view of Table 4, we observe that all three methods give comparable results and all three methods are even more robust with respect to the penalized parameter β . The same conclusion is valid for the next example for higher dimensions.

TABLE 5. Smooth solution in 100 dimensions

β	e_{L^2}	e_{H^1}	e_{H^2}
Deep Nitsche Method			
50	8.611e-4	5.014e-3	2.075e-2
500	7.795e-4	4.466e-3	1.826e-2
5000	3.224e-3	5.977e-3	2.098e-2
50000	2.291e-3	5.368e-3	2.023e-2
Deep Ritz Method			
50	1.590e-3	4.800e-3	1.869e-2
500	7.028e-3	8.984e-3	2.355e-2
5000	7.992e-4	4.609e-3	2.126e-2
50000	2.291e-3	5.368e-3	2.023e-2
Least-Squares Method			
50	5.689e-3	7.716e-3	2.374e-2
500	8.759e-4	4.845e-3	2.235e-2
5000	1.118e-3	3.915e-3	1.662e-2
50000	1.121e-3	6.444e-3	2.740e-2

In the second example, we consider a smooth solution in 100 dimensions.

$$u(x) = \exp\left(\frac{1}{100} \sum_{i=1}^{100} x_i\right), \quad x \in (0, 1)^{100}$$

with a pure Dirichlet boundary condition. We compute f and g_D by (2.1). The exact solution u is approximated by a neural network with five residual blocks and 100 hidden nodes per fully connected layer, and the number of trainable parameters is 111201. We report the relative errors in Table 5. It shows that our method has potential to work for rather high dimensions.

4. CONCLUSION

Based on Nitsche's idea and representing the trial functions by deep neural network, we propose a new method to deal with the complicated boundary conditions. The test examples show that the method has the following advantages:

- (1) It deals with the mixed boundary conditions in a variational way without significant extra costs and it fits well with the stochastic gradient descent method.
- (2) It works on the problems in low dimensions as well as high dimensions. It also has potential to work for problem in rather high dimensions.
- (3) The method is less sensitive to the penalized parameter, by contrast to that for the traditional trial space [8]. This is more pronounced in high dimensions.

We also systematically compare Deep Nitsche Method with Deep Ritz Method and least-squares method for regular as well as singular solution, for low dimensional problems as well as high dimensional problems. It seems that the new method is comparable to these two methods, while it is slightly more accurate for singular solution. There are still several issues we have not addressed such as the influence of the network structures and a systematical method to improve the accuracy, which will be pursued in our future work.

REFERENCES

1. I. Babuška, U. Banerjee, and J.E. Osborn, *Surveys of meshless and generalized finite element method: a unified approach*, Acta Numer. **12** (2003), 1–125.
2. J. Berg and K. Nystrom, *A unified deep artificial neural network approach for partial differential equations in complex geometries*, Neural Computing **317** (2018), 28–41.
3. J.H. Bramble and A. Schatz, *Rayleigh-Ritz-Galerkin methods for Dirichlet's problem using subspaces without boundary conditions*, Comm. Pure Appl. Math. **XXIII** (1970), 353–675.
4. E. Burman and P. Zunino, *Numerical approximation of large contrast problems with the unfitted Nitsche method*, Frontiers in Numerical Analysis-Durham 2010, J. Blowey and M. Jensen Eds., Springer-Verlag Berlin Heidelberg, 2012, pp. 227–281.
5. W. E, J.Q. Han, and A. Jentzen, *Deep learning-based numerical methods for high-dimensional parabolic partial differential equations and backward stochastic differential equations*, Commun. Math. Stat. **5** (2017), 349–380.
6. W. E and B. Yu, *The Deep Ritz Method: a deep-learning based numerical algorithm for solving variational problems*, Commun. Math. Stat. **6** (2018), 1–12.
7. Y. Goodfellow, I. Bengio and A. Courville, *Deep Learning*, MIT Press, Cambridge, 2016.
8. M. Griebel and M.A. Schweitzer, *A particle-partition of unit method part V: boundary conditions*, Geometric Analysis and Nonlinear Partial Differential Equations, S. Hildebrandt eds., Springer-Verlag Berlin Heidelberg, 2003, pp. 519–542.
9. J.Q. Han, A. Jentzen, and W. E, *Solving high-dimensional partial differential equations using deep learning*, Proc. Natl. Acad. Sci. **115** (2018), no. 34, 8505–8510.
10. K.M. He, X.Y. Zhang, S.Q. Ren, and J. Sun, *Deep residual learning for image recognition*, In: IEEE Conference on Computer Vision and Pattern Recognition (CVPR) (2016), 770–778.
11. J. Khoo, J. Lu, and L. Ying, *Solving parametric pde problems with artificial neural networks*, 2017, arXiv: 1707.03351.
12. D.P. Kingma and J. Ba, *Adam: A method for stochastic optimization*, 2014, arXiv preprint arXiv:1412.6980; Published as a conference paper at ICLR 2015.
13. H.N. Mhaskar, *When is approximation by Gaussian networks necessarily a linear process?*, Neural Networks **17** (2004), 989–1001.
14. J. Nitsche, *Über ein Variationsprinzip zur Lösung von Dirichlet-Problemen bei Verwendung von Teilräumen, die keinen Randbedingungen unterworfen sind*, Abh. Math. Sem. Univ. Hamburg **36** (1971), 9–15.
15. J. Sirignano and K. Spiliopoulos, *DGM: A deep learning algorithm for solving partial differential equations*, J. Comput. Phys. **375** (2018), 1339–1364.
16. G. Strang and G.J. Fix, *An Analysis of the Finite Element Method*, Prentice-Hall, Inc., Englewood Cliffs, N. J., 1973.

INSTITUTE OF COMPUTATIONAL MATHEMATICS AND SCIENTIFIC/ENGINEERING COMPUTING, AMSS,
CHINESE ACADEMY OF SCIENCES, NO. 55, EAST ROAD ZHONG-GUAN-CUN, BEIJING 100190,
CHINA, AND SCHOOL OF MATHEMATICAL SCIENCES, UNIVERSITY OF CHINESE ACADEMY OF SCI-
ENCES, BEIJING 100049, CHINA

E-mail address: `liaoyulei19@mailsucas.ac.cn`

LSEC, INSTITUTE OF COMPUTATIONAL MATHEMATICS AND SCIENTIFIC/ENGINEERING COMPUT-
ING, AMSS, CHINESE ACADEMY OF SCIENCES, NO. 55, EAST ROAD ZHONG-GUAN-CUN, BEIJING
100190, CHINA, AND SCHOOL OF MATHEMATICAL SCIENCES, UNIVERSITY OF CHINESE ACADEMY
OF SCIENCES, BEIJING 100049, CHINA

E-mail address: `mpb@lsec.cc.ac.cn`